Available online at https://ganitjournal.bdmathsociety.org/

GANIT: Journal of Bangladesh Mathematical Society

GANIT*J. Bangladesh Math. Soc.* 43.1 (2023) 63–75
DOI: https://doi.org/10.3329/ganit.v43i1.67859

Finite element simulation on MHD Free Convection in a Square Enclosure with Elliptical Shaped Obstacle

Muhammad Sajjad Hossain[a], C. K. Sarder[a], K. E. Hoque[a], M.Z.I. Bangalee[b], M. M. Billah[a,*], M. Ashraf Uddin[c]

[a]*Department of Arts and Sciences, Ahsanullah University of Science and Technology (AUST), Dhaka- 1208, Bangladesh*
[b]*Department of Applied Mathematics, University of Dhaka, Dhaka- 1000, Bangladesh*
[c]*Department of Mathematics, Bandarban Cantonment Public School and College, Bandarban – 4600, Bangladesh*

ABSTRACT

The study is focused on the magneto-hydrodynamic (MHD) free convection flow phenomenon with varied positions of elliptical obstacle in a square enclosure. Cavity's base wall is uniformly heated, and the enclosure has a cold top wall and insulated side walls. Three diverse positions of elliptical obstacle, such as, left-bottom elliptical obstacle (LBEO), right-bottom elliptical obstacle (RBEO) and right-top elliptical obstacle (RTEO) are deemed for the analysis inside the enclosure. Additionally, the elliptical barriers are evenly heated. The mathematical model was created using a few governing equations with boundary conditions, and the non-dimensional governing equations were then solved using a Galerkin finite element formulation. Various elliptical obstacles and the parametric research study for the wide range of Hartmann number ($0 \leq Ha \leq 100$), fixed Rayleigh number ($Ra = 10^3$) and Prandtl number ($Pr = 0.7$) have been used in this case. The results have been demonstrated for various positions of elliptical obstacle (LBEO, RBEO and RTEO) using the streamline phase, isotherms, and average Nusselt number in the cavity. The average Nusselt number was found to drop for the pattern of LBEO and RBEO when the Hartman number was raised, but increased for RTEO pattern.

Received: January 2, 2023 **Accepted:** May 12, 2023 **Published Online:** July 15 , 2023

Keywords: Free convection; MHD; Finite element method; Square cavity; Elliptical obstacle

1. Introduction

The attributes of heat transfer, natural convection flow studies in cavities have received significant attention by the pioneering interest of researchers because of numerous technological applications in nature and the area of engineering.

*Corresponding Author. *Email Address:*mmb.edu@gmail.com

Interesting situations could arise when a magnetic field has been imposed externally to a shear and buoyancy-driven container containing an electrically conducting fluid, providing stability to the flow and inhibiting heat transfer. A lot of numerical and experimental investigations have been completed to analyze the flow characteristics in the different shaped cavity without and with obstacle by the researchers because those geometries have practical applications in engineering and industrial fields. A few mentionable fields are cooling of electronic devices, air conditioning, design of solar collectors, thermal design of building, chemical processing equipment, drying technologies etc. Some researchers recently examined heat transmission within enclosures containing different fluids with various geometrical parameters and boundary conditions, as covered in the following literature.

Vázquez et al. [1] studied the simulation of a large eddy upon the natural convection within a confined square cavity to find the turbulent regime of fluid flow on boundary layers of the vibrant walls and laminar flow on the horizontal walls. Jani et al. [2] examined free convection amid a magnetic field in the cavity of a square and showed that both the vigor of the mesmeric field and Rayleigh number play a momentous role in temperature distribution and flow pattern in the cavity. The conjugated natural heat transfer by convection occurs in a divided differentially heated square cavity. was performed by Carvalho and De Lemos [3]. The results demonstrated that Nusselt number is decreased for larger values of k_s / k_f as well as for the increased material porosity. Zhuo and Zhong [4] examined the turbulent natural convection in a square cavity to use an LES-based filter-matrix Boltzmann model. They found that proper minimization of the higher-order terms of Ra could expand numeric accuracy of the model for greater Ra convective flow. Heat flow visualization and entropy creation lying on natural convection in inclined square cavities was studied by Basak et al. [5]. It was discovered that heat transfer rates occur for $\varphi = 15^\circ$ cavities in the convection dominating mode for $Ra = 10^5$ by reducing entropy production. Hossain and Alim [6] performed natural convection inside the trapezoidal cavity where magnetic field is applied. It was demonstrated that the average and local Nusselt number at non-uniform heating of the cavity's bottom wall depended on dimensionless parameters as well as tilt angles. Hossain et al. [7] also performed impact of circular block on magnetic-natural convection inside the trapezoidal cavity. Fluid-solid interaction in natural convection heat transfer in a square cavity was studied by Jamesahar et al. [8] for examining the actions of the membrane and the convective heat transfer of the cavity for several non-dimensional parameters. Ezan and Kalfa [9] investigated transient natural convection of freezing water for finding heat transfer in a square cavity. The noticed that natural convection became noticeable and took various forms during the early stages of the phase change process. Lyubimova and Zubova [10] studied nonlinear regimes of convection of binary fluid in square cavity. The outcomes indicate that the time of instability's onset depend on the singular Rayleigh number. Khatamifar et al. [11] studied conjugate natural convection heat transfer in a square cavity. It was discovered that the average Nusselt number for the whole range of Rayleigh numbers was little impacted by the partition position. A semi-elliptical fin inserted in a lid-driven square cavity to find the improvement in thermal performance, was examined by Razera et al. [12]. Analysis of heat flow on natural convection in a trapezoidal cavity along with non-uniformly heated triangular block was investigated by Hossain et al. [13]. It was discovered that non-dimensional factors, tilt angles, and non-uniformly heated triangular blocks had a substantial impact on heat transfer rates. Natural convection in a trapezoidal cavity with magnetic field and cooled triangular obstacle of different orientations was also analyzed by Hossain et al. [14]. Wang et al. [15] studied non-oberbeck-boussinesq effects due to large temperature differences in a differentially heated square cavity. it had been analyzed that the thermal and velocity boundary layers both thicken near the hot plate while becoming thinner near the cold plate. A rotating cylinder inside a square enclosure on natural convection was analyzed by Hassanzadeh et al. [16] and they found faster spinning speeds at lower Rayleigh numbers. Al-Kouz et al. [17] performed rarefied gaseous flows in an oblique wavy square cavity. It was found that the tilt angle has a significant impact on the flows of heat transmit. Hossain et al. [18] studied different types of aspect ratio of heated triangular block on natural convection within a trapezoidal cavity. They also used porus matrix and magnetic field in the cavity. They showed that aspect ratio of heated triangular block has a significant impact on local and average Nusselt numbers. The effect of polymer additives and viscous dissipation on natural convection in a square cavity was performed by Chauhan et al. [19]. They observed that the average Nusselt number steadily grew with the Weissenberg number as well as for low Rayleigh numbers. Furthermore, the average Nusselt number was decreased when the polymer extensibility and polymer viscosity ratio was increased. Hossain et al. [20] investigated the effect of various positions of a heated cylinder with magnetic field on natural convection in a square cavity. They analyzed that local Nusselt number decreased for the LBC and LTC configurations but increased for the RBC and RTC configurations with the increase of Hartmann number. Turkyilmazoglu [21] studied the exponential non-uniform wall heating on natural convection in a square cavity and the heating location was expected to have a greater influence on heat transmission if the center of heating was closer to the upper horizontal wall.

According to the scientist's knowledge, no research has been done yet on magneto-hydrodynamic free convection in a square cavity with elliptical obstacle where the geometrical outcome for the characteristics of the heat transport is

essential in order to understand the industrial functions. The temperature region is specified by isotherms whereas the flow field has been displayed by the streamlines. The airflow in the cavity is taken into account for calculating using the Prandtl number $(\mathrm{Pr} = 0.7)$. The investigation has been done on three heated elliptical obstacle configurations (LBEO, RBEO and RTEO) for the range of Ha and Ra on flow and thermal field through square cavity.

2. Physical Model

A steady and two-dimensional square cavity with magnetic field (B0) has been studied in the present model, shown in the Fig. 1. The dimension of the cavity is defined by its height and length and is denoted by H (H = 0.6). The size of elliptical obstacle is measured by the width and height parameters a, b called the semi-major and semi-minor axes where a = 0.15 and b = 0.1. The elliptical obstacle position´s for LBEO = (0.25, 0.2), RBEO = (0.35, 0.2) and RTEO = (0.25, 0.4) is considered inside the enclosure. Fig. 1 depicts the left-bottom elliptical obstacle (LBEO). It is presumed that the vertical walls are adiabatic while the bottom wall is uniformly heated. The top wall is also presumed as cold temperature. The gravity (g) always is operated in the downward direction. The fluid of the enclosure is treated Newtonian and laminar. Furthermore, the boundary walls of the enclosure are measured as no-slip.

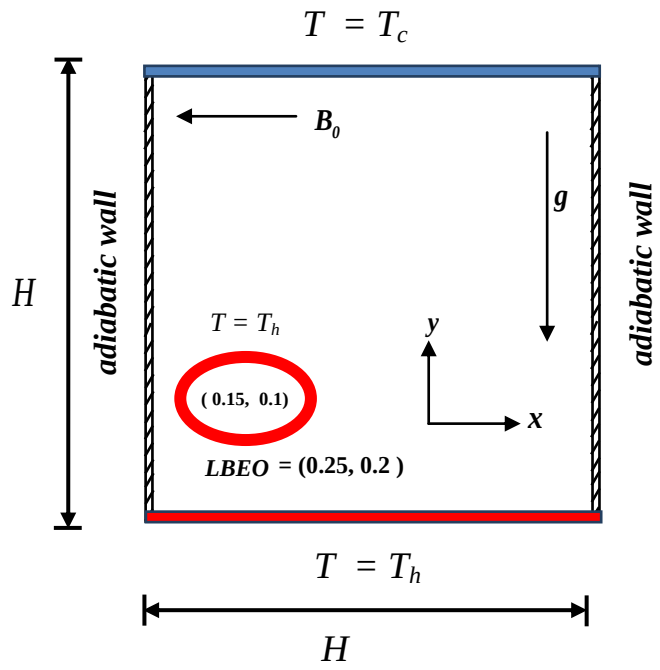

Fig. 1: Simplified diagram of the physical system

3. Governing equations

In the present study, the fluid for two-dimensional square enclosure is viscous, incompressible. The thermo-physical properties of the fluid flow are constant excluding density variation which varies the Boussinesq approximation. Viscous dissipation and radiation´s effect are ignored here. Now, the equations for continuity, momentum and energy with a magnetic field in x-direction for the present study in dimensional form are given below [2][6] [7][22-24] [25] :

$$\frac{\partial u}{\partial x}+\frac{\partial v}{\partial y}=0 \tag{1}$$

$$u\frac{\partial u}{\partial x}+v\frac{\partial u}{\partial y}=-\frac{1}{\rho}\frac{\partial p}{\partial x}+\nu\left(\frac{\partial^2 u}{\partial x^2}+\frac{\partial^2 u}{\partial y^2}\right) \tag{2}$$

$$u\frac{\partial v}{\partial x}+v\frac{\partial v}{\partial y}=-\frac{1}{\rho}\frac{\partial p}{\partial y}+\nu\left(\frac{\partial^2 v}{\partial x^2}+\frac{\partial^2 v}{\partial y^2}\right)+\rho g\beta(T-T_c)-\sigma\beta_0^2 v \tag{3}$$

$$u\frac{\partial T}{\partial x}+v\frac{\partial T}{\partial y}=\frac{k}{\rho c_p}\left(\frac{\partial^2 T}{\partial x^2}+\frac{\partial^2 T}{\partial y^2}\right) \tag{4}$$

where x and y both are horizontal and vertical coordinates, u and v are velocity components, T and p are temperature and pressure. Volumetric thermal expansion coefficient, kinematic viscosity, density, acceleration due to gravity, magnitude of the magnetic field and dynamic viscosity are expressed respectively by the symbols $\beta, v, \rho, g, B_0, \sigma$.

The variables to make the governing equations (1) to (4) non-dimensional are as follows:

$$\begin{aligned} &X=\frac{x}{H},\ Y=\frac{y}{H},\ U=\frac{uH}{\alpha},\ V=\frac{vH}{\alpha},\quad P=\frac{pH^2}{\rho\alpha^2},\quad \theta=\frac{T-T_c}{T_h-T_c},\\ &Ha=B_0H\sqrt{\frac{\sigma}{\mu}},\quad \Pr=\frac{\nu}{\alpha},\quad Ra=\frac{g\beta(T_h-T_c)H^3}{\alpha\nu} \end{aligned} \tag{5}$$

Now, the non-dimensional forms of the governing equations are:

$$\frac{\partial U}{\partial X}+\frac{\partial V}{\partial Y}=0 \tag{6}$$

$$U\frac{\partial U}{\partial X}+V\frac{\partial U}{\partial Y}=-\frac{\partial P}{\partial X}+\Pr\left(\frac{\partial^2 U}{\partial X^2}+\frac{\partial^2 U}{\partial Y^2}\right) \tag{7}$$

$$U\frac{\partial V}{\partial X}+V\frac{\partial V}{\partial Y}=-\frac{\partial P}{\partial Y}+\Pr\left(\frac{\partial^2 V}{\partial X^2}+\frac{\partial^2 V}{\partial Y^2}\right)+Ra\Pr\theta-Ha^2\Pr V \tag{8}$$

$$U\frac{\partial \theta}{\partial X}+V\frac{\partial \theta}{\partial Y}=\left(\frac{\partial^2 \theta}{\partial X^2}+\frac{\partial^2 \theta}{\partial Y^2}\right) \tag{9}$$

where *X* and *Y* both are dimensionless horizontal and vertical coordinates, U and V are dimensionless velocity components in *X* and *Y* directions, θ and P are the dimensionless temperature and pressure, Pr, *Ha* and *Ra* are respectively Prandtl number, Hartmann number and Rayleigh number.

The dimensionless boundary conditions for solving the equations (6) – (9) are:

$U=0,\ V=0,\ \theta=0;$ on the top wall

$U=0,\ V=0,\ \frac{\partial\theta}{\partial n}=0;$ on the left and right (vertical) walls

$U=0,\ V=0,\ \theta=1;$ on the bottom wall

$U=0,\ V=0,\ \theta=1;$ on the elliptical obstacle

For the calculation of the rate of heat transfer, the local Nusselt number (Nu_{local}) along the heated surface is $Nu_{local}=-\frac{\partial\theta}{\partial n}$, where n is the dimensionless distances either *X* or *Y* direction acting normal to the surface of the solid obstacle and the average Nusselt number along the heated surface of the enclosure is defined as, $Nu_{av}=-\frac{1}{H}\int_0^H Nu_{local}\,dS$, where $\frac{\partial\theta}{\partial n}=\sqrt{\left(\frac{\partial\theta}{\partial X}\right)^2+\left(\frac{\partial\theta}{\partial Y}\right)^2}$ and *H* and *S* are respectively the length of the heated surface and the non-dimensional coordinate along the elliptical surface.

4. Solution Technique

For the current study, the Galerkin technique of finite elements [26, 27] has been applied to solve dimensionless governing equations using its boundary conditions. Because of mass conservation, the equation of continuity is used as a restraint. The distribution of pressure can be determined using this limit.. This penalty restraint's large values immediately satisfy the continuity equation. A basis set is then used to expand the components for velocity (U, V) and also for temperature (θ). The non-linear residue equations are then generated by the Galerkin finite element system. Three factors, the integrals in these equations are evaluated using Gaussian quadrature. To find the coefficients of the expansion, the nonlinear residual equations are solved using the Newton-Raphson method [28]. The convergence for the solutions is took as read because the relative error for each erratic between consecutive iterations is recorded for the convergence reason ε, such that $\left(\psi^{n+1}-\psi^{n} \leq 10^{-5}\right)$, where n is the number of iterations and Ψ is a function of U, V, θ and Tecplot have been used for numerical-graphical results and post-processing.

5. Code Validation

The validation of the physical model is an essential part for the accuracy of the numerical technique. So, the present numerical result is demonstrated against a documented numerical research work for validation the code. Now, the numerical calculation for the present work was solved with Pr = 0.7, *Ha* = 50 and *Ra* = 10^3 for streamlines and isotherms within a square cavity for pure natural convection. The results are compared with the reported paper by Jani et al. [2] and obtained good agreement, which is demonstrated in Fig. 2.

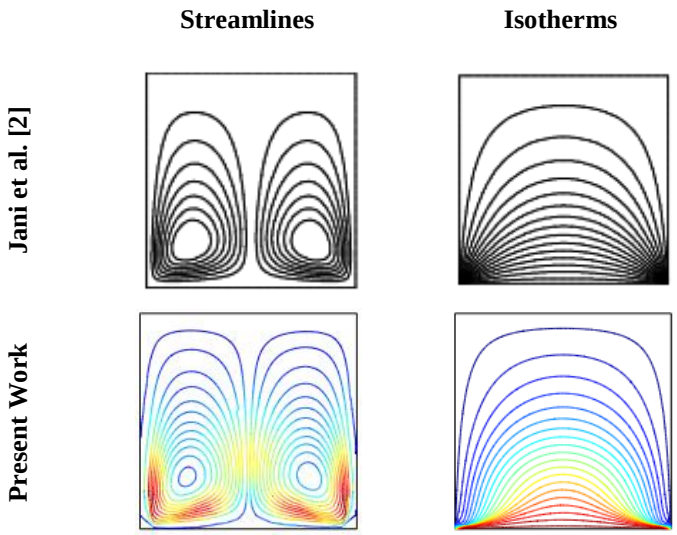

Fig. *2*: Comparisons of present study and Jani et al.[2] for stream function and isotherms with Pr = 0.71, Ha= 50 and Ra = 10^3.

6. Grid Independence Test

The geometry which studied is a square enclosure with elliptic shaped block while a number of grid refinement tests are carried out in this geometry with LBEO at Pr = 0.7, Ha = 50 and *Ra* = 10^3 to obtain the sufficiency of mesh scheme and to make sure that the solutions are grid independent. This is determined by the computational results of Nusselt number and solution time. There are seven different non-uniform grids in total. For the grid independence tests, a certain number of nodes and elements, such as, 5793 nodes, 846 elements; 9313 nodes, 1380 elements; 15711 nodes, 2360 elements; 22584 nodes, 3384 elements; 27524 nodes, 4144 elements; 34934 nodes, 5284 elements, 40121 nodes, 6082 elements are demonstrated in the table 1(see also Fig. 3a). From the above study, 27524 nodes, 4144 elements are chosen to get the approved result in the simulation. In addition, the current mesh configuration of the enclosure is also shown in Fig. 3b.

Table 1: Grid Independence Tests at Pr = 0.7, Ha =50 and $Ra = 10^3$ for LBEO

Nodes	5793	9313	15711	22584	27524	34934	40121
Elements	846	1380	2360	3384	4144	5284	6082
Time	2.534	3.815	5.71	9.284	12.438	17.205	18.7875
Nu_{av}	0.346819	0.3466	0.356818	0.3569	0.3569	0.0.3569	0.356901

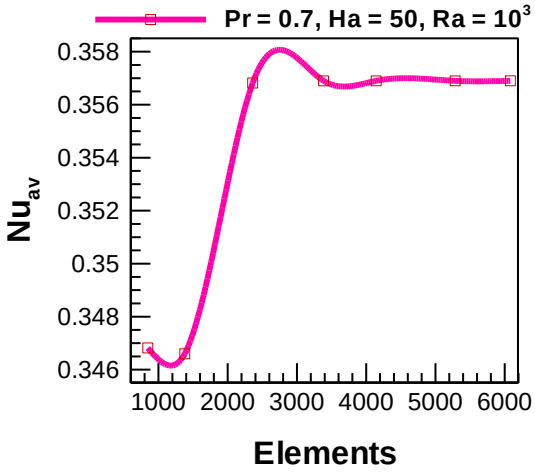

Fig. 3a*:* Grid Independence at Pr = 0.7, *Ha* = 50 and $Ra = 10^3$ for LBEO

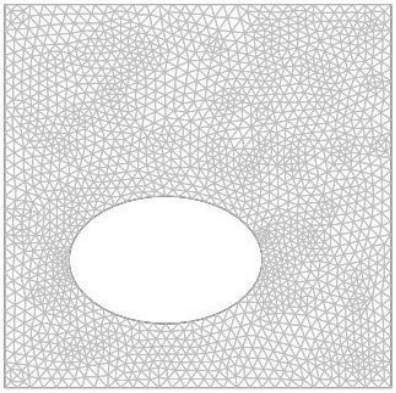

Fig. 3b*:* The mesh pattern

7. Discussion on the results

The numerical results of the flow of fluid on magnetic-free convection within a square enclosure with insider elliptical obstacle for different orientations have been presented here. The enclosure having insider elliptical obstacle is considered for an electric conductive fluid with Pr = 0.7 (Jani et al. [2]) where *Ha* = 0 - 100 and $Ra = 10^3$. The numerical results of the present study are focused on flow and temperature fields, which started with streamlines and temperature contours (isotherms) inside the enclosure. Furthermore, the representative distributions of heat transfer rates, such as, average Nusselt number with the heated bottom wall, and average bulk temperature of the fluid in the enclosure has also been analyzed here.

7.1 Streamlines and isotherms: Effect of Ha and Elliptical obstacles

The flow characteristics analyses for this problem have been performed in the form of streamlines and temperature contours which is presented in isotherms for several ranges of parameters such as Prandtl number (Pr = 0.7), Harmann number (*Ha* = 0 - 100) and Rayleigh number ($Ra = 10^3$) along with various orientations of elliptical obstacle and is demonstrated in the Fig. 4 – Fig. 12. The influence of the Hartmann number Ha (Ha = 0, 50, 100) on streamlines and isotherms are presented in Fig. 4 – Fig. 6 respectively for left bottom elliptical obstacle pattern (LBEO). From the Fig. 4, it is seen that, in the absence of Hartmann number, one big clockwise circulation cell around the elliptical obstacle is formed inside the cavity and one vortex is formed at the left-top wall of the cavity and furthermore one tiny vortex is formed at the left-bottom wall of the cavity, which produced a shear force on a flow field. When the Hartmann number is increased to 50, two vortices has been formed at the center of the eddy circulation cell of the cavity (see Fig. 5). It is also observed from Fig. 5 that left-top vortex becomes smaller than the previous one (see Fig.4) and left-bottom vortex has been increased in size a little,which happens due to high flow strength inside the enclosure. As increased the Hartmann number to 100, the quantity of circulating eddies increased due to the fact of buoyancy force and magnetic-flow strength. Besides this, a little significant change of the vortices are viewed inside the cavity. Two vortices are seen inside the eddy cell whose size are decreasing. But also smaller left-top vortex and bigger left-bottom vortex are seen in the Fig. 6. As seen in the Fig. 4 – Fig. 6, the isotherms are akin to as linear in addition to nonlinear close to the top wall and bottom wall by way of the raise of Hartmann number. Furthermore, as the Hartmann number, Ha, increases, so does

the temperature of the flow field, implies that the magnetic parameter *Ha* has significant impact on fluid flow resistance due to its high magnetic strength.

Figs. 7 – Fig. 9 display the effect of Hartmann number *Ha* (Ha = 0, 50, 100) for right bottom elliptical obstacle (RBEO) on the velocity and temperature distributions for $Ra = 10^3$ and Pr = 0.7. It is watched from Fig. 7 that when Ha = 0, that is, in absence of magnetic field, a small recirculation cell appears at the center of the square enclosure and one vortex has been formed at the right-top corner of the enclosure. When magnetic field (Ha = 50) is applied, one additional vortex has been formed at the center part of the cavity and another one vortex has been appeared at the lower right part of the cavity and the right-top vortex is reduced in size (see the Fig. 8). For highest Ha = 100, any significant major changes is not seen but right-top right vortex becomes dense which is indicated by the colored blue (see the Fig. 9). As observed in Fig. 7- Fig. 9, the isotherms are parallel to the top wall of the square cavity but the non-linearity effect is found in the near bottom wall of the square cavity.

Figs. 10 – Fig. 12 illustrate the streamlines and isotherms for the right top elliptical obstacle (RTEO) with variations of Hartmann number *Ha* (Ha = 0, 50, 100) while $Ra = 10^3$ and Pr = 0.7. From Fig. 10, it is found one cell which is formed at the center portion of the square cavity in absence of magnetic field. One tiny vortex is appeared at right-top corner of the cavity which is shoed by densely colored and another vortex has formed at the lower right part of the cavity. By appling magnetic field, Ha = 50, it has been watched from Fig. 11 that two vortices is occurred in the center of the cavity and right-top corner vortex becomes slighter than the before. Furthermore, streamlines are densely colored near the boundary walls as well as the elliptical obstacle of the enclosure (see Fig. 11). When we increased Hartmann number to 100, only change has been viewed on the streamlines where right-top vortex now become larger than before (see Fig. 12). For the isotherms, it has been displayed from Fig. 10 – Fig. 12 that, isotherm lines is linear and dense at the top of the elliptical obstacle of the enclosure and to the cold top wall and also non-linear lines are observer at the bottom of the elliptical obstacle of the enclosure.

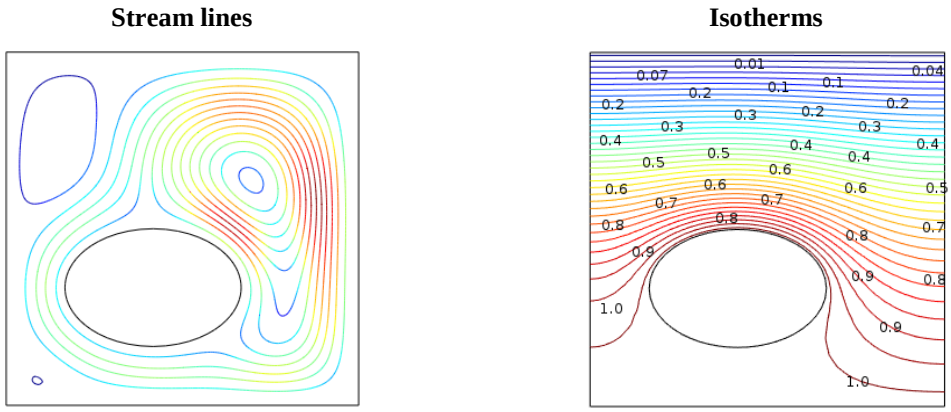

Fig. 4: streamlines and isotherms for Ha= 0 and for Ra = 10^3 for LBEO

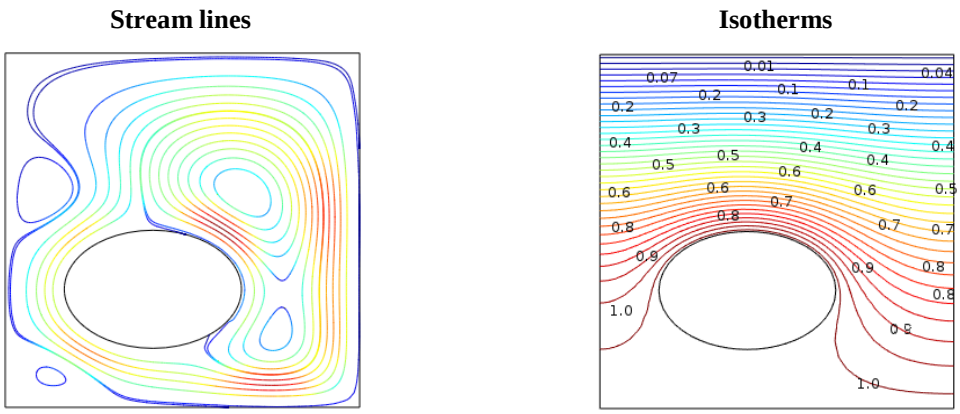

Fig. 5: streamlines and isotherms for Ha= 50 and for Ra = 10^3 for LBEO

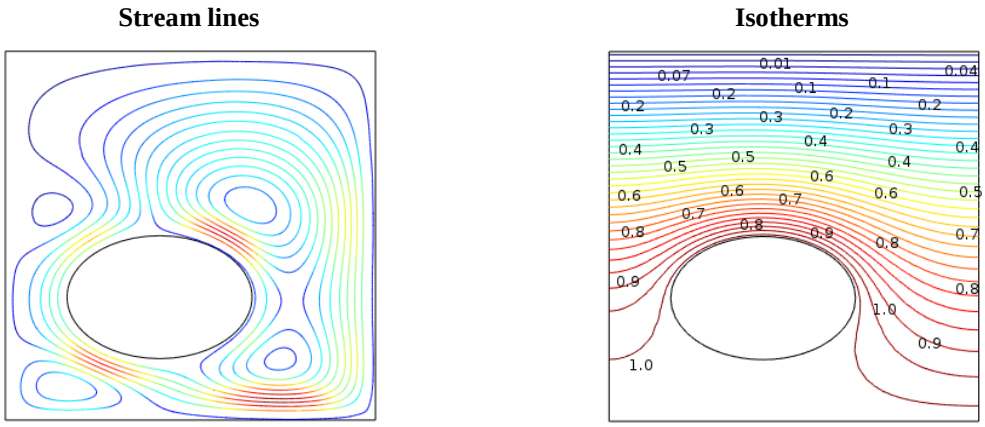

Fig. 6: streamlines and isotherms for Ha = 100 and for Ra = 10^3 for LBEO

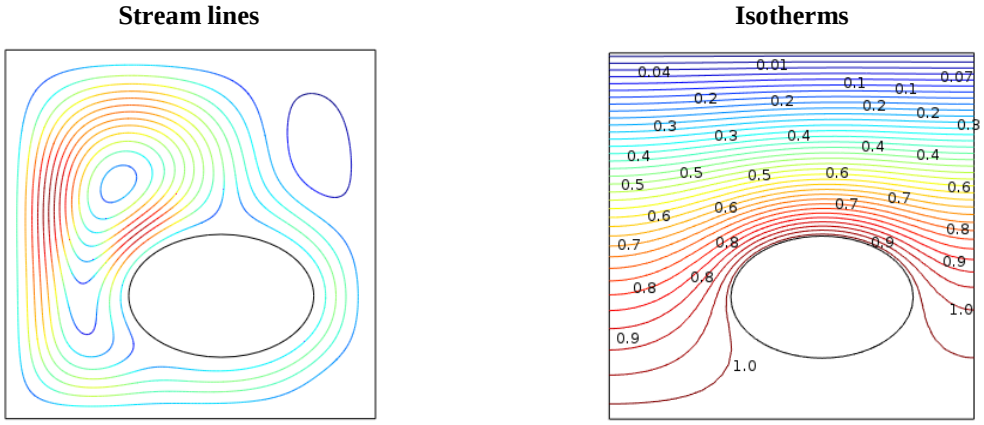

Fig. 7: streamlines and isotherms for Ha = 0 and for Ra = 10^3 for RBEO

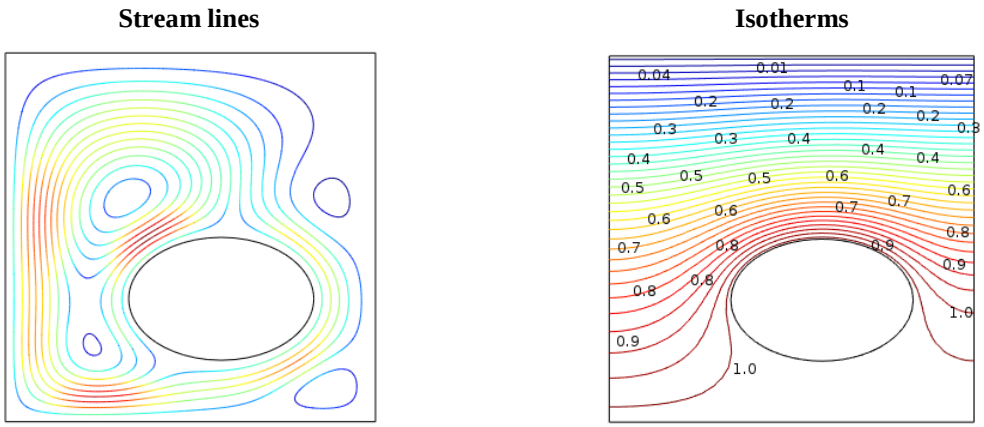

Fig. 8: streamlines and isotherms for Ha = 50 and for Ra = 10^3 for RBEO

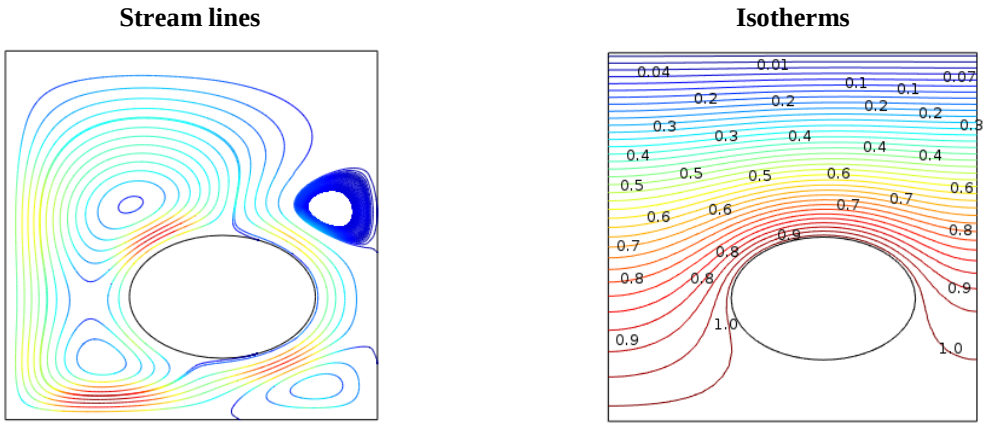

Fig. 9: streamlines and isotherms for Ha = 100 and for Ra = 10^3 for RBEO

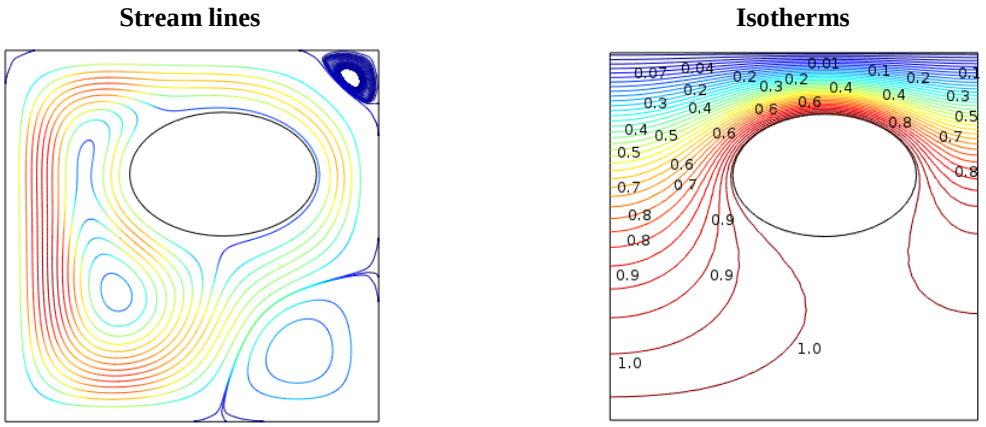

Fig. 10: streamlines and isotherms for Ha = 0 and for Ra = 10^3 for RTEO

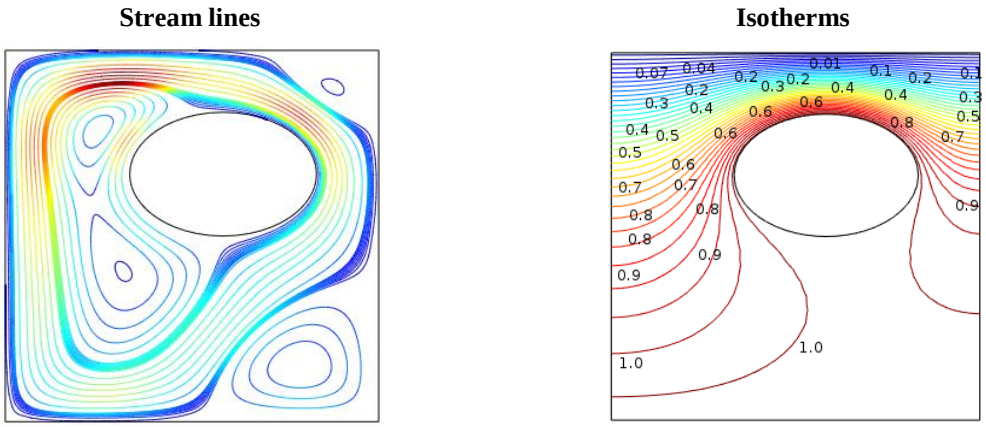

Fig. 11: streamlines and isotherms for Ha = 50 and for Ra = 10^3 for RTEO

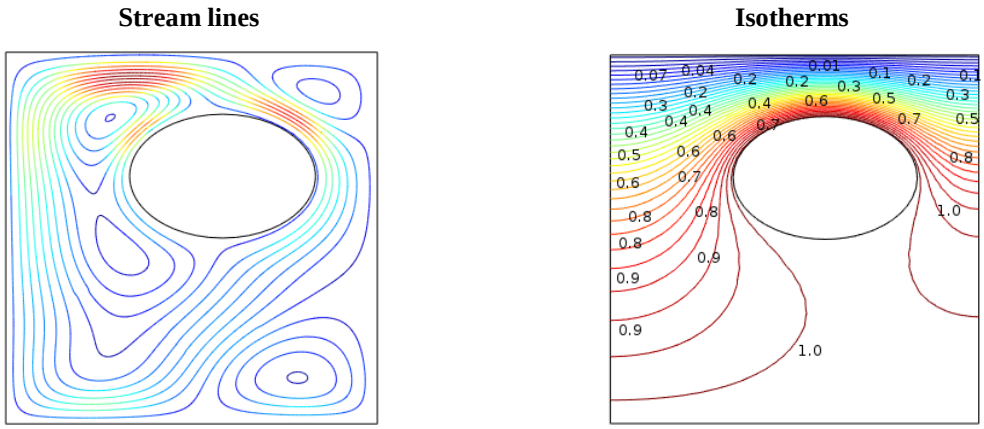

Fig. 12: streamlines and isotherms for Ha = 100 and for Ra = 10^3 for RTEO

7.2 Heat transfer rates: average Nusselt number vs Ha

The effects of Hartmann number on the heat transfer rates as well as average Nusselt number for different LBEO, RBEO and RTEO configurations have been displayed in the Fig. 13 where Pr = 0.7, Ra = 10^3 and the graph is marked by the colored red, green and blue respectively. From the Fig. 13 it was viewed for LBEO that the average Nusselt number at the uniform heating of bottom wall of the enclosure was the highest when magnetic field was absent due to convective heat transfer inside the enclosure and decreases when Hartman number was increased to 50 and remained linear up to Ha = 100 for LBEO and RBEO configuration which also shows the conduction dominated region in the cavity..But for RTEO Configuration, the average Nusselt number was the lowest due to nonexistence of magnetic field (Ha = 0) and highest at Ha = 100.

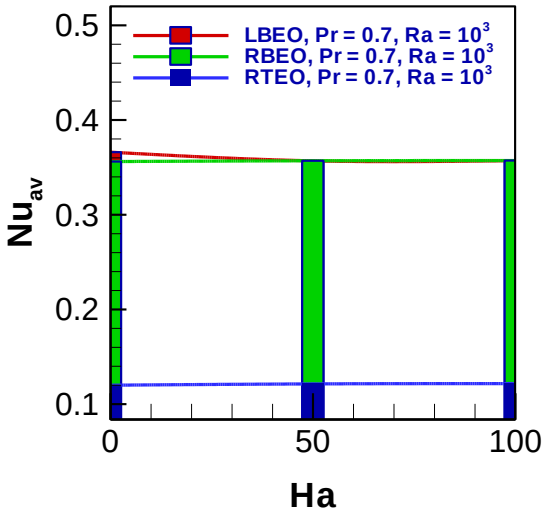

Fig. 13: Effect of Ha on Nu_{av} for diverse LBEO, RBEO and RTEO when Ra = 10^3

8. Conclusions

The flow simulation work is carried out by the use of an easiness algorithm of Galerkin residual technique to analyze the flow of fluid and heat transfer on magneto-hydrodynamic free convection with elliptical obstacle within square enclosure in the current investigation. The present inquiries have been focused in the form of streamlines, isotherms,

average Nusselt number having elliptical obstacle for an assortment of *Ha* and fixed *Pr* and *Ra*. The following findings have been formed based on the analysis:

- The mechanism of heat transfer, flow characteristics and isotherm distributions within the enclosure fully depended upon an assortment of heated elliptical obstacle, Prandlt number (Pr), Rayleigh number (*Ra*) and Hartmann number (*Ha*).
- Hartmann numbers have significant impact on fluid flow resistance due to its high magnetic strength. Moreover, the effect of Magnetic parameter *Ha* on streamlines and isotherms are remarkable. The eddies in the streamlines are reduced and the thermal current surrounding the heated body is thin with elevating *Ha.*
- Due to the free convection parameter *Ra*, buoyancy-induced vortex in the streamlines is increased and thermal layer near the heated surface becomes thick; which implies the strong convection flow.
- Dense streamlines were seen for the raise of Hartmann number. Furthermore, the quantities of vortices were increased inside the streamlines for different elliptical obstacle placement inside the cavity as well as the augment of Hartmann number; therefore, the elliptical obstacle has also a significant effect on the flow and temperature fields.
- Linear patterns of isotherm lines were seen at the top of the elliptical obstacle and near the cooled top wall and non-linear patterns are formed under the elliptical obstacle and bottom wall of the enclosure for LBEO and RBEO pattern figure. But dense linear isotherm patterns were observed for the RTEO pattern figure at the top of the elliptical obstacle and near the cooled top wall of the enclosure.
- The average Nusselt number at the uniform heating of bottom wall of the enclosure was the highest when magnetic field was absent and decreases when Hartman number was increased to 50 and remained linear up to Ha = 100 for the figure of LBEO and RBEO. For RTEO pattern, the average Nusselt number was lowest for nonexistence of magnetic field (Ha = 0) and Nu_{av} was increased when *Ha* was increased to 50. When *Ha* increased to 100 then the highest heat transfer rate was found. Furthermore, it is summarized that buoyant motion and heat transfer rate upgrades due to increasing shear rate for the expansion of Hartmann number.

List of Abbreviations

LBEO Left-bottom elliptical obstacle
RBEO Right-bottom elliptical obstacle
RTEO Right-top elliptical obstacle

Conflict of Interests

All authors declare that there is no conflict of interest regarding the publication of this paper.

Acknowledgements

All authors want to express their gratitude to the anonymous referees for their precious comments and constructive suggestions of the manuscript and also want to give thankfulness to the Department of Arts and Sciences, AUST, Dhaka, for giving computing facility to finish this research work.

Funding

All authors declare that there was no external fund available for this research work.

References

[1] Vázquez M.S.; Vicente W.; Martínez E.; Barrios E, Large eddy simulation of a confined square cavity with natural convection based on compressible flow equations. International Journal of Heat and Fluid Flow**,** 32(5): 876-888(2011).
[2] Jani S.; Mahmoodi M.; Amini M., Magnetohydrodynamic Free Convection in a Square Cavity Heated from Below and Cooled from Other Walls. International Journal of Mechanical and Mechatronics Engineering, 7(4): 750-755(2013).

[3] Carvalho P. H. S.; De Lemos M. J. S., Turbulent free convection in a porous square cavity using the thermal equilibirum model. International Communications in Heat and Mass Transfer**,** 49:10-16(2013).
[4] Zhuo C.; Zhong C., LES-based filter-matrix lattice Boltzmann model for simulating turbulent natural convection in a square cavity. International Journal of Heat and Fluid Flow, 42:10-22(2013).
[5] Basak T.; Singh A. K.; Sruthi T. P. A.; Roy S., Finite element simulations on heat flow visualization and entropy generation during natural convection in inclined square cavities. International Communications in Heat and Mass Transfer, 51:1-8(2014).
[6] Hossain M. S.; Alim M. A. MHD free convection within trapezoidal cavity with non-uniformly heated bottom wall. International Journal of Heat and Mass Transfer, 69: 327-336(2014).
[7] Hossain M. S.; Alim M. A.; Kabir K. H., Numerical Analysis on MHD Natural Convection within Trapezoidal Cavity Having Circular Block. Science and Education Publishing, 4(5):161-168(2016).
[8] Jamesahar E.; Ghalambaz M.; Chamkha A. J., Fluid–solid interaction in natural convection heat transfer in a square cavity with a perfectly thermal-conductive flexible diagonal partition. International Journal of Heat and Mass Transfer, 100: 303-319(2016).
[9] Ezan M. A.; Kalfa M., Numerical investigation of transient natural convection heat transfer of freezing water in a square cavity. International Journal of Heat and Fluid Flow, 61(Part B):438-448(2016).
[10] Lyubimova T.; Zubova N., Onset and nonlinear regimes of convection of binary fluid with negative separation ratio in square cavity heated from above. International Journal of Heat and Mass Transfer, 106: 1134-1143(2017).
[11] Khatamifar M.; Lin W.; Armfield S.W.; Holmes D.; Kirkpatrick M. P., Conjugate natural convection heat transfer in a partitioned differentially-heated square cavity. International Communications in Heat and Mass Transfer, 81:92-103(2017).
[12] Razera A. L.; Da Fonseca R.J.C.; Isoldi L. A., Constructal design of a semi-elliptical fin inserted in a lid-driven square cavity with mixed convection. International Journal of Heat and Mass Transfer, 126(Part B):81-94(2018).
[13] Hossain M. S.; Alim M. A.; Andallah L. S., Numerical Investigation of Natural Convection Flow in a Trapezoidal Cavity with Non-uniformly Heated Triangular Block Embedded Inside. Journal of Advances in Mathematics and Computer Science, 28(5):1-30(2018).
[14] Hossain M. S.; Alim M. A.; Andallah L. S., A comprehensive analysis of natural convection in a trapezoidal cavity with magnetic field and cooled triangular obstacle of different orientations. AIP Conference Proceedings, 2121: 030003-1-030003-10(2019).
[15] Wang Q.; Xia S. N.; Yan R.; Sun D. J.; Wan Z. H., Non-Oberbeck-Boussinesq effects due to large temperature differences in a differentially heated square cavity filled with air. International Journal of Heat and Mass Transfer, 128: 479-491(2019).
[16] Hassanzadeh R.; Rahimi R.; Khosravipour A.; Mostafavi S.; Pekel H., Analysis of natural convection in a square cavity in the presence of a rotating cylinder with a specific number of roughness components. International Communications in Heat and Mass Transfer, 116:1-18(2020).
[17] Al-Kouz W.; Saleem K. B.; Chamkha A., Numerical investigation of rarefied gaseous flows in an oblique wavy sided walls square cavity. International Communications in Heat and Mass Transfer, 116:1-16(2020).
[18] Hossain M. S.; Alim M. A.; Andallah L. S., Numerical Simulation of MHD Natural Convection Flow Within Porous Trapezoidal Cavity with Heated Triangular Obstacle. International Journal of Applied and Computational Mathematics, 6(166): 1-27(2020).
[19] Chauhan A.; Sahu P.M.; Sasmal C., Effect of polymer additives and viscous dissipation on natural convection in a square cavity with differentially heated side walls. International Journal of Heat and Mass Transfer. **2021,** 175:1-15(2021).
[20] Hossain M. S.; Fayz-Al-Asad Md.; Mallik M. S. I.; Yavuz M.; Alim M. A.; Basher Md. K. Numerical study of the effect of a heated cylinder on natural convection in a square cavity in the presence of a magnetic field. Mathematical and Computational Applications, 27(4) (58): 1-17(2022).
[21] Turkyilmazoglu M., Exponential nonuniform wall heating of a square cavity and natural convection. Chinese Journal of Physics, 77:2122-2135(2022).
[22] Djeumegni J. S.; Lazard M. Le Dez V.; Kamdem H. T. T., Radiative heat transfer in a 2D semi-transparent gray medium with a centered inner square cavity. International Journal of Heat and Mass Transfer, 149: 1-19(2020).
[23] Şahin B., Effects of the center of linear heating position on natural convection and entropy generation in a linearly heated square cavity. International Communications in Heat and Mass Transfer**,** 117:1-18(2020).

[24] Liao C. C.; Li W. K. Assessment of the magnetic field influence on heat transfer transition of natural convection within a square cavity. Case Studies in Thermal Engineering, 28(101638):1-11 (2021).
[25] Fayz-Al-Asad Md.; Alam Md. N.; Rashad A.M.; Sarker Md. M. A. Impact of undulation on magneto-free convective heat transport in an enclosure having vertical wavy sides. International Communications in Heat and Mass Transfer, 127(105579): 1-7(2021).
[26] Taylor C.; Hood P. A numerical Solution of the Navier-Stokes Equations Using Finite Element Technique. Computer and Fluids. 1973, 1(1),73-100(1973).
[27] Dechaumphai P., Finite Element Method in Engineering, Chulalongkorn University Press, 2nd edition, Bangkok, (1999)
[28] Reddy, J. N., An Introduction to the Finite Element Method. McGraw-Hill, New York (1985).